

# Optimal Non-Coherent Detector for Ambient Backscatter Communication System

Sudarshan Guruacharya, *Member, IEEE*, Xiao Lu, *Member, IEEE*, and Ekram Hossain, *Fellow, IEEE*

**Abstract**—The probability density function (pdf) of the received signal of an ambient backscatter communication system is derived, assuming that on-off keying (OOK) is performed at the tag, and that the ambient radio frequency (RF) signal is white Gaussian. The pdf of the received signal is then utilized to design two different types of non-coherent detectors. The first detector directly uses the received signal to perform a hypothesis test. The second detector first estimates the channel based on the observed signal and then performs the hypothesis test. Test statistics and optimal decision threshold of the detectors are derived. The energy detector is shown to be an approximation of the second detector. For cases where the reader is able to avoid or cancel the direct interference from the RF source (e.g., through successive interference cancellation), a third detector is given as a special case of the first detector. Numerical results show that both the first and the second detectors have the same bit error rate (BER) performance, making the second detector preferable over the first detector due to its computational simplicity.

**Index Terms**—Product of complex Gaussians, ambient backscatter communication, non-coherent detector

## I. INTRODUCTION

Ambient backscatter communication has been introduced as an energy-efficient alternative to low-power communication systems. As shown in Fig. 1, in this system, a tag communicates with a reader by modulating and reflecting the ambient radio frequency (RF) signals from surrounding RF sources, such as TV stations, cellular and WiFi networks. This eliminates active RF components at the tag, leading to simpler circuitry and lower power consumption [1]–[5].

Many challenges abound in this emerging technology. One of the challenges in this area is in the design of the signal detector at the reader. The reasons for this are: 1) the wireless channel for an ambient backscatter communication system is not a traditional point-to-point channel, 2) the nature of RF signal (such as bandwidth, transmit power, waveform) exploited by the system is generally unknown to the reader and it should be considered as a random signal, and 3) because of the previous reason, the reader lacks the training symbols required to estimate the channel parameters. As such, the channel state information (CSI) is unknown to the reader.

A number of recent works [6]–[11] have tried to address this problem. The common feature of all these works is that the detector is designed in ignorance of the statistics of the

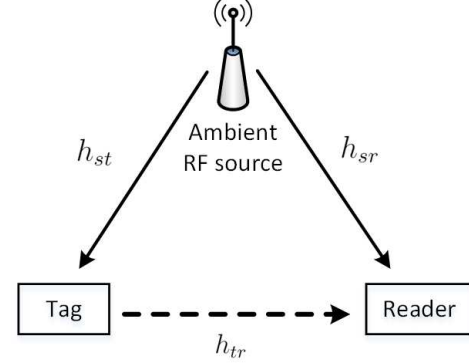


Fig. 1: Ambient backscatter system consisting of RF signal source, a passive tag, and a reader.

received signal when the channel is unknown. When the statistics of the received signal is used, the channel is assumed to be known, leading to a semi-coherent detector requiring training symbols to determine the detection threshold. Various differential coding schemes have been used in an attempt to bypass this essential ignorance. However, despite their claims, references [6]–[10] have been unsuccessful in their effort to construct a truly non-coherent detector. To the best of our knowledge, reference [11] is the only paper that has succeeded in presenting a truly non-coherent detector by using differential Manchester coding, where the CSI is not required at the reader. However, with Manchester coding, the data rate is halved. When the RF source employs orthogonal frequency-division multiplexing (OFDM), references [12]–[14] have exploited the structure of OFDM waveform to construct the required detector.

Recently, the authors in [15] derived the statistics for the sum of a circularly symmetric complex Gaussian (CSCG) vector with the product of a CSCG scalar and another CSCG vector. In this letter, we apply these results to derive the statistics of received signal at the reader of an ambient backscatter communication system, which is then utilized to construct an optimal non-coherent detector. Three different detectors are presented, and their performances are studied.

**Notations:** Lower/upper bold face letters denote vectors/matrices;  $|\cdot|$ ,  $\mathbf{I}_N$ ,  $\|\cdot\|$  denote magnitude, identity matrix of size  $N$ , and Euclidean norm;  $p(\cdot)$  and  $\Pr(\cdot)$  probability density function (pdf) and probability operator, respectively.  $\mathcal{CN}(0, \sigma^2 \mathbf{I}_N)$  denotes a CSCG distribution with zero-mean and co-variance matrix  $\sigma^2 \mathbf{I}_N$ ;  $\gamma(z, a)$  denotes lower incomplete gamma function.

S. Guruacharya is with the Department of Electrical and Computer Engineering, New York Institute of Technology, Old Westbury, NY, USA (e-mail: srguruach@nyit.edu).

X. Lu is with the Department of Electrical and Computer Engineering, University of Alberta, AB, Canada (e-mail: lu9@ualberta.ca).

E. Hossain is with the Department of Electrical and Computer Engineering, University of Manitoba, MB, Canada (e-mail: ekram.hossain@umanitoba.ca).

## II. SYSTEM MODEL

Consider a simple ambient backscatter configuration which consists of an ambient RF source, a passive tag, and a reader as shown in Fig. 1. The RF energy broadcasted by the source is received both by the tag and the receiver. The passive tag can reflect the incoming RF signal to the reader by changing its impedance. As such, the tag is capable of transmitting binary symbols to the reader by choosing whether or not to backscatter the incident RF energy. The symbols “0” and “1” correspond to the tag’s non-backscattering and backscattering state. The reader senses the changes to its received signal and decodes the transmitted symbols of the tag.

The baseband signal received at the tag at the  $n$ -th sampling instance is

$$x[n] = h_{st}s[n], \quad (1)$$

where  $s[n]$  is the unknown random RF signal and  $h_{st}$  represents the channel coefficient between the RF source and the tag. Since the thermal noise at the tag is very small, we will follow the convention where this noise is omitted. We assume that  $s[n]$  is a complex white Gaussian signal. That is, the signals are independent and identically distributed (i.i.d.) as  $\mathbf{s} \sim \mathcal{CN}(0, \sigma_s^2 \mathbf{I}_N)$  where  $\mathbf{s} = (s[0], \dots, s[N-1])^T$ . Commonly used modulation schemes, such as OFDM and code-division multiplexing (CDM), are approximately white Gaussian in time domain. Due to the central limit theorem, this is also a good approximation when the exploited RF signal results from the superposition of signals from multiple RF sources. Likewise, we assume that we have a scatter-rich environment allowing us to model  $h_{st}$  as Rayleigh fading channel whose distribution is given by  $h_{st} \sim \mathcal{CN}(0, \sigma_{st}^2)$ .

Let us denote the  $k$ -th binary symbol of the tag as  $b_k \in \{0, 1\}$ , which is assumed to be equiprobable. The tag transmits data at a slower rate than the RF signal. As such, we can assume that  $b_k$  is a constant over the interval of observation where  $N$  samples are collected. Assuming that the tag uses non-return to zero (NRZ) line code to represent the bits via simple on-off keying (OOK), the signal backscattered by the tag is given by

$$x_b[n] = \alpha b_k x[n], \quad (2)$$

where  $\alpha$  is a scaling term related to the scattering efficiency and antenna gain of the tag. Without any loss of generality, we will assume  $\alpha = 1$ .

The baseband signal received at the reader corresponding to the  $k$ -th tag symbol  $b_k$  is

$$\begin{aligned} y[n] &= h_{sr}s[n] + h_{tr}x_b[n] + w[n], \\ &= (h_{sr} + b_k h_{st} h_{tr})s[n] + w[n]. \end{aligned} \quad (3)$$

Here  $h_{sr}$  is the channel coefficient between the RF source to the reader, while  $h_{tr}$  is the channel coefficient between the tag to the reader. We will assume both  $h_{sr}$  and  $h_{tr}$  to be Rayleigh fading channels; thus  $h_{sr} \sim \mathcal{CN}(0, \sigma_{sr}^2)$  and  $h_{tr} \sim \mathcal{CN}(0, \sigma_{tr}^2)$ . Likewise,  $\mathbf{w} \sim \mathcal{CN}(0, \sigma_w^2 \mathbf{I}_N)$  is the i.i.d. additive complex white Gaussian noise, where  $\mathbf{w} = (w[0], \dots, w[N-1])^T$ . Hence, depending on the value of  $b_k$ , the signal received at the reader is

$$y[n] = \begin{cases} h_0 s[n] + w[n] & \text{if } b_k = 0 \\ h_1 s[n] + w[n] & \text{if } b_k = 1 \end{cases}, \quad (4)$$

where  $h_0 = h_{sr}$  and  $h_1 = h_{sr} + h_{st} h_{tr}$ .

Let  $\mathbf{y} = (y[0], \dots, y[N-1])^T$  be a vector of  $N$  observations sampled at the reader. In order to construct an optimal detector, we need to know what the distribution of  $\mathbf{y}$  is. However, the answer to this question depends on the coherence time of the wireless channels. In the simplest instance, we will assume that the channel coherence time is equal to the observation time so that the channel gains  $h_{st}$ ,  $h_{tr}$ , and  $h_{sr}$  remain constant during the  $N$  observations, but may vary in different coherence intervals independently. However, during non-coherent detection, the reader does not possess the CSI. As such, the detector has to take the randomness of the wireless channels into account. Another complication is that since any two samples  $y[m]$  and  $y[n]$  share the same random channel values for any  $m \neq n$ , this implies that  $y[m]$  and  $y[n]$  are no longer independent of each other.

## III. PDF OF $\mathbf{y}$

In this section, we will derive the pdf of  $\mathbf{y}$  when  $b_k \in \{0, 1\}$ , which is required during the design of non-coherent detector. We will use the integral function  $\mathcal{I}_L(z; a, b)$  and its properties, reviewed in the **Appendix**, to express the pdf of  $\mathbf{y}$  in a convenient form. Let us denote the energy of the signal  $\mathbf{y}$  by  $z = \|\mathbf{y}\|^2$ . Also, let the squared magnitude of channel coefficients be denoted as  $v_0 = |h_0|^2$  and  $v_1 = |h_1|^2$ .

When  $b_k = 0$ , the conditional pdf of  $y[n]$  given  $v_0$  is

$$y[n] | v_0 \sim \mathcal{CN}(0, v_0 \sigma_s^2 + \sigma_w^2), \quad (5)$$

where the pdf of  $v_0$  is given by the exponential distribution

$$p_{V_0}(v_0) = \frac{1}{\sigma_{sr}^2} e^{-v_0/\sigma_{sr}^2}. \quad (6)$$

De-conditioning with respect to  $v_0$ , the pdf of  $\mathbf{y}$  can be directly written as [15, Eqn 4]

$$p_{\mathbf{Y}}(\mathbf{y} | b_k = 0) = K_0 \mathcal{I}_N(z; \sigma_w^2, \sigma_{sr}^2 \sigma_s^2), \quad (7)$$

where  $K_0 = e^{\frac{\sigma_w^2}{\sigma_{sr}^2 \sigma_s^2}} / (\pi^N \sigma_{sr}^2 \sigma_s^2)$  is a constant.

When  $b_k = 1$ , the pdf of  $y[n]$  conditioned on  $v_1$  is

$$y[n] | v_1 \sim \mathcal{CN}(0, v_1 \sigma_s^2 + \sigma_w^2). \quad (8)$$

Hence, the conditional pdf of vector  $\mathbf{y}$  is

$$p_{\mathbf{Y}}(\mathbf{y} | v_1) = \frac{1}{(\pi(v_1 \sigma_s^2 + \sigma_w^2))^N} \exp\left(-\frac{z}{v_1 \sigma_s^2 + \sigma_w^2}\right). \quad (9)$$

From [15, Eqn 15], the pdf of  $v_1$  is

$$p_{V_1}(v_1) = \frac{1}{\sigma_{st}^2 \sigma_{tr}^2} \exp\left(\frac{\sigma_{sr}^2}{\sigma_{st}^2 \sigma_{tr}^2}\right) \mathcal{I}_1(v_1; \sigma_{sr}^2, \sigma_{st}^2 \sigma_{tr}^2). \quad (10)$$

De-conditioning (9), we have

$$p_{\mathbf{Y}}(\mathbf{y} | b_k = 1) = \int_0^\infty p_{\mathbf{Y}}(\mathbf{y} | v_1) p_{V_1}(v_1) dv_1. \quad (11)$$

Let  $u = v_1 \sigma_s^2 + \sigma_w^2$ , then substituting (9) and (10) into (11), we obtain

$$\begin{aligned} p_{\mathbf{Y}}(\mathbf{y} | b_k = 1) &= K_1 \int_{\sigma_w^2}^\infty \frac{e^{-z/u}}{u^N} \\ &\quad \times \mathcal{I}_1\left(\frac{u - \sigma_w^2}{\sigma_s^2}; \sigma_{sr}^2, \sigma_{st}^2 \sigma_{tr}^2\right) du, \end{aligned} \quad (12)$$

where  $K_1 = e^{\frac{\sigma_{sr}^2}{\sigma_{st}^2 \sigma_{tr}^2}} / (\pi^N \sigma_{st}^2 \sigma_{tr}^2 \sigma_s^2)$  is a constant.

Using the definition given in (28) for  $\mathcal{I}_1(\cdot)$  in (12) and interchanging the order of integration, we obtain an alternative expression for  $p_{\mathbf{Y}}(\mathbf{y}|b_k = 1)$  as

$$p_{\mathbf{Y}}(\mathbf{y}|b_k = 1) = K_1 \int_{\sigma_{sr}^2}^{\infty} \frac{1}{t} \exp \left\{ - \left( \frac{t}{\sigma_{st}^2 \sigma_{tr}^2} - \frac{\sigma_w^2}{\sigma_s^2 t} \right) \right\} \times \mathcal{I}_N(z; \sigma_w^2, \sigma_s^2 t) dt. \quad (13)$$

#### IV. OPTIMAL NON-COHERENT DETECTOR

Here we will give two approaches to construct a detector for  $b_k$ . The first approach directly utilizes the pdf of  $\mathbf{y}$ . The second approach estimates  $v$  and then performs the hypothesis test, given the estimate of  $v$ . A third detector is also given as a special case of the first detector, assuming that the direct link interference has somehow been nullified.

##### A. First Detector: Direct Approach

The simplest approach in constructing a detector is to directly use the pdf of  $\mathbf{y}$  to derive the test statistics and decision threshold. Thereby, given the observation vector  $\mathbf{y}$ , the detector needs to perform a binary hypothesis test where  $H_0 : \mathbf{y} = h_0 \mathbf{s} + \mathbf{w}$  and  $H_1 : \mathbf{y} = h_1 \mathbf{s} + \mathbf{w}$ . The optimal non-coherent detector is given by the likelihood ratio test (LRT) detector. We have the LRT given by

$$\frac{p_{\mathbf{Y}}(\mathbf{y}|b_k = 1)}{p_{\mathbf{Y}}(\mathbf{y}|b_k = 0)} \underset{H_0}{\overset{H_1}{\gtrless}} 1. \quad (14)$$

From (7) and (12), the test statistics for log-LRT is

$$\Lambda_1 = \log \int_{\sigma_w^2}^{\infty} \frac{e^{-z/u}}{u^N} \mathcal{I}_1 \left( \frac{u - \sigma_w^2}{\sigma_s^2}; \sigma_{sr}^2, \sigma_{st}^2 \sigma_{tr}^2 \right) du - \log \mathcal{I}_N(z; \sigma_w^2, \sigma_{sr}^2 \sigma_s^2), \quad (15)$$

with the optimal decision threshold as  $\theta_1^* = \log(\frac{K_0}{K_1})$ , or

$$\theta_1^* = \frac{\sigma_w^2}{\sigma_{sr}^2 \sigma_s^2} - \frac{\sigma_{sr}^2}{\sigma_{st}^2 \sigma_{tr}^2} + \log \left( \frac{\sigma_{st}^2 \sigma_{tr}^2}{\sigma_{sr}^2} \right). \quad (16)$$

Let  $\hat{b}_k$  be the decision made by the detector, then the detector will decide  $\hat{b}_k = 0$  if  $\Lambda_1 < \theta_1^*$ , otherwise  $\hat{b}_k = 0$  if  $\Lambda_1 > \theta_1^*$ .

##### B. Second Detector: Indirect Approach

Another approach to construct a non-coherent detector is as follows: let  $h = h_{sr} + b_k h_{st} h_{tr}$  be the unknown channel that depends on  $b_k$  and let  $v = |h|^2$ . For a given  $v$ , we know that

$$p_{\mathbf{Y}}(\mathbf{y}|v) = \frac{1}{(\pi(v\sigma_s^2 + \sigma_w^2))^N} \exp \left( - \frac{z}{v\sigma_s^2 + \sigma_w^2} \right).$$

The maximum log-likelihood estimate of  $v$  is

$$v^* = \arg \max_{v \geq 0} \log p_{\mathbf{Y}}(\mathbf{y}|v), \quad (17)$$

which after some basic calculus is given by

$$v^* = \left( \frac{z}{N\sigma_s^2} - \frac{\sigma_w^2}{\sigma_s^2} \right)_+, \quad (18)$$

where  $(x)_+ = \max(0, x)$ . Using  $v^*$  we can decide whether  $H_0 : v = |h_0|^2$  or  $H_1 : v = |h_1|^2$  is true. The LRT detector is given by

$$\frac{p_V(v^*|b_k = 1)}{p_V(v^*|b_k = 0)} \underset{H_0}{\overset{H_1}{\gtrless}} 1. \quad (19)$$

Here  $p_V(v|b_k = 0)$  is given by (6) and  $p_V(v|b_k = 1)$  is given by (10). Hence, the log-LRT will give us the test statistics

$$\Lambda_2 = \frac{v^*}{\sigma_{sr}^2} + \log \mathcal{I}_1(v^*; \sigma_{sr}^2, \sigma_{st}^2 \sigma_{tr}^2), \quad (20)$$

with an optimal decision threshold

$$\theta_2^* = \log \left( \frac{\sigma_{st}^2 \sigma_{tr}^2}{\sigma_{sr}^2} \right) - \frac{\sigma_{sr}^2}{\sigma_{st}^2 \sigma_{tr}^2}. \quad (21)$$

As done previously, the detector will decide  $\hat{b}_k = 0$  if  $\Lambda_2 < \theta_2^*$ , otherwise  $\hat{b}_k = 0$  if  $\Lambda_2 > \theta_2^*$ .

##### C. Discussion

- 1) In the indirect approach, if we neglect  $\sigma_w^2$  and  $\log \mathcal{I}_1(v^*; \sigma_{sr}^2, \sigma_{st}^2 \sigma_{tr}^2)$  in the test statistics, the second detector will reduce to a simple *energy detector* with  $\Lambda_2 \approx z/N\sigma_{sr}^2 \sigma_s^2$ . Hence, the energy detector will have similar behavior and limitations as the second detector.
- 2) When  $\sigma_w^2/\sigma_{sr}^2 \sigma_s^2$  is negligible, then  $\theta_1^* = \theta_2^*$ .

##### D. Special Case: Detection After Interference Nullification

In some cases, the reader can avoid or cancel the direct interference from the RF source. For example, if the reader can decode the symbols transmitted by the RF source, then it can cancel the interference from the received backscattered signal. Likewise, the backscattered signal can be modulated to appear in a different frequency band, free from direct interference [13]. Assuming that direct RF interference is nullified, we can construct an optimal detector for this special case using the results obtained so far. When  $b_k = 0$ , there is only noise at the reader. Thus, the pdf of  $\mathbf{y}$  is simply

$$p_{\mathbf{Y}}(\mathbf{y}|b_k = 0) = \frac{e^{-z/\sigma_w^2}}{(\pi\sigma_w^2)^N}. \quad (22)$$

When  $b_k = 1$  the pdf of  $\mathbf{y}$  is given by (12), where we set  $\sigma_{sr}^2 = 0$ , which after applying (30), we obtain

$$p_{\mathbf{Y}}(\mathbf{y}|b_k = 1) = \frac{2}{\pi^N \sigma_{st}^2 \sigma_{tr}^2 \sigma_s^2} \times \int_{\sigma_w^2}^{\infty} \frac{e^{-z/u}}{u^N} \mathcal{K}_0 \left( 2\sqrt{\frac{u - \sigma_w^2}{\sigma_{st}^2 \sigma_{tr}^2 \sigma_s^2}} \right) du, \quad (23)$$

where  $\mathcal{K}_0$  is the zeroth-order modified Bessel function of the second kind. The log-LRT in (14) will yield the test statistics

$$\Lambda_3 = \frac{z}{\sigma_w^2} + \log \int_{\sigma_w^2}^{\infty} \frac{e^{-z/u}}{u^N} \mathcal{K}_0 \left( 2\sqrt{\frac{u - \sigma_w^2}{\sigma_{st}^2 \sigma_{tr}^2 \sigma_s^2}} \right) du, \quad (24)$$

with an optimal decision threshold

$$\theta_3^* = \log \left( \frac{\sigma_{st}^2 \sigma_{tr}^2 \sigma_s^2}{2\sigma_w^2} \right) - (N-1) \log \sigma_w^2. \quad (25)$$

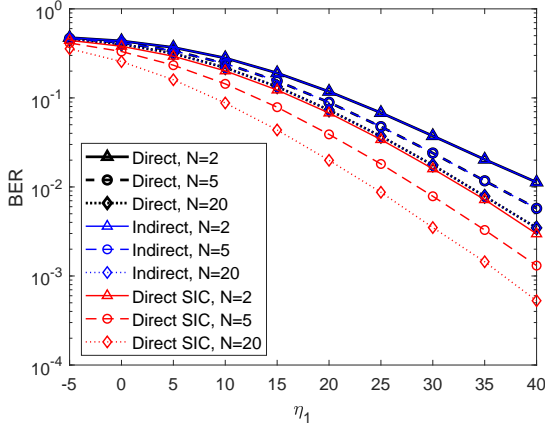


Fig. 2: BER versus SIR ( $\eta_1$ ) given INR  $\eta_2 = 0$  dB.

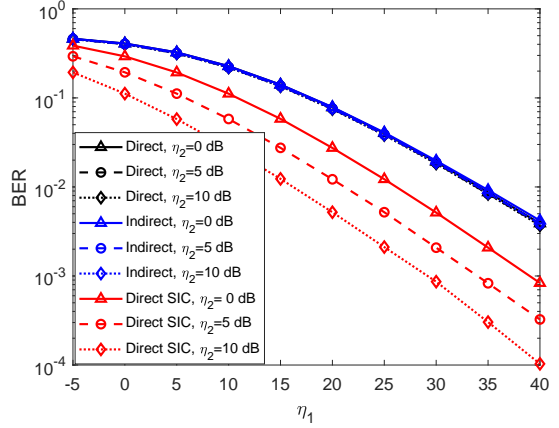


Fig. 4: BER versus SIR ( $\eta_1$ ) given  $N = 10$ .

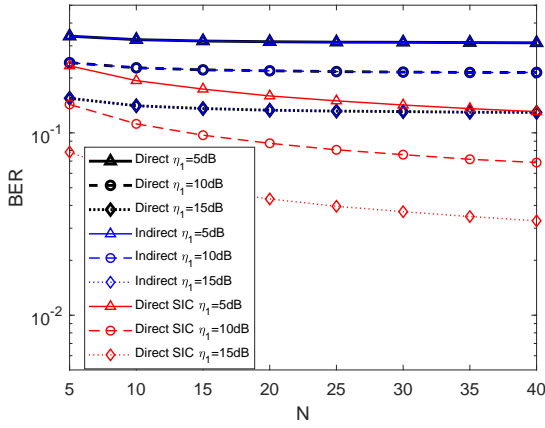


Fig. 3: BER versus  $N$  given INR  $\eta_2 = 0$  dB.

## V. NUMERICAL EVALUATION

Let the decision made by the detector for the  $k$ -th transmitted bit be denoted as  $\hat{b}_k$ , then the bit error rate (BER) of the detector is defined as

$$\text{BER} = \frac{1}{2} \left[ \Pr(\hat{b}_k = 0 | b_k = 1) + \Pr(\hat{b}_k = 1 | b_k = 0) \right]. \quad (26)$$

Since the signal from the direct source-to-reader path appears as an interference to the desired signal from the source-tag-reader path, in the following, we will plot the BER of the non-coherent detector with respect to the signal-to-interference-plus-noise ratio (SINR). The SINR is defined as

$$\eta = \frac{\sigma_{st}^2 \sigma_{tr}^2 \sigma_s^2}{\sigma_{sr}^2 \sigma_s^2 + \sigma_w^2} = \frac{\eta_1}{1 + \frac{1}{\eta_2}}, \quad (27)$$

where  $\eta_1 = \sigma_{st}^2 \sigma_{tr}^2 / \sigma_{sr}^2$  is the signal-to-interference ratio (SIR) while  $\eta_2 = \sigma_{sr}^2 \sigma_s^2 / \sigma_w^2$  is the interference-to-noise ratio (INR). Clearly, when  $\eta_2$  is large, we have  $\eta \approx \eta_1$ . Given these definitions, we can re-express the optimal threshold for the detectors as  $\theta_1^* = 1/\eta_2 - 1/\eta_1 + \log(\eta_1)$ ,  $\theta_2^* = \log(\eta_1) - 1/\eta_1$ , and  $\theta_3^* = \log(\eta/2) - (N-1) \log \sigma_w^2$ .

In practice, the tag and the reader are separated by a short distance while the RF source is located far away from both the tag and the reader. As such, we can approximately consider the

tag and the reader to be equidistant from the RF source. Hence,  $\sigma_{st}^2 = \sigma_{sr}^2$  and  $\eta_1 = \sigma_{tr}^2$ . In the Monte Carlo simulations, we set  $\eta_2 = 0$  dB while changing  $\eta_1$  by changing  $\sigma_{tr}^2$ . Each point in a plot is constructed using  $10^6$  Monte Carlo instances. To speed up the simulation, integrals in (15), (20) and (24) are evaluated by first creating a lookup table for  $z = 0, \Delta, 2\Delta, \dots, z_{\max}$ , where  $\Delta$  is the table's step size. The lookup table is then used to interpolate the integral value for required  $z \in [0, z_{\max}]$  during the Monte Carlo simulation. We set  $\Delta = 0.1$  and  $z_{\max} = 2000$  and use linear interpolation. If  $z > z_{\max}$ , we use (33) as an approximation for  $\mathcal{I}_L(z)$  in (20), or numerically evaluate the integrals.

In Fig. 2, we plot the BER versus SIR. We find that both the first and second detectors (labeled as ‘‘Direct’’ and ‘‘Indirect’’, respectively) have the same performance, while the third detector (labeled as ‘‘Direct SIC’’) unsurprisingly outperforms the first two detectors. We observe that with increasing SIR, the BER decreases. As we vary the sample size  $N$ , we observe that for a given SIR, the BER decreases with increasing  $N$ . However, as  $N$  increases, the BER performance saturates and does not improve beyond a certain point. The change in BER with respect to sample size  $N$  is more obvious in Fig. 3, where the contrast in the behavior of first/second and third detectors is distinctly observed. Lastly, in Fig. 4 the BER versus SIR plot is given again, but this time we vary the INR  $\eta_2$  by changing  $\sigma_s^2$ . We observe that for given  $\eta_1$ , there is no change in the performance of the first/second detector. This is because, for given  $\eta_1$ , as  $\eta_2$  increases, SINR  $\eta \rightarrow \eta_1$  a constant. However, the performance of the third detector improves with increasing  $\sigma_s^2$  because for this case  $\eta_2$  is always zero. As such, increasing  $\sigma_s^2$  increases the SNR, improving its performance.

## VI. CONCLUSION

We have derived the pdf of the received signal at the tag of an ambient backscatter communication system, which was then used to design two different types of detectors. The energy detector was shown to be an approximation of the second detector, while the interference-free case was also studied. Numerical results showed that both the first and second detector have the same performance. Also, there was only

a limited improvement in the performance of non-coherent detectors with an increase in sample size. However, the second detector is computationally simpler than the first detector. In practice, lookup tables are essential for fast processing. Extension of the work to different channel models, higher modulation schemes, and multiple antenna systems will be an interesting research direction.

#### APPENDIX: INTEGRAL FUNCTION $\mathcal{I}_L(z; a, b)$

The integral function  $\mathcal{I}_L(z; a, b)$  is defined as [15]

$$\mathcal{I}_L(z; a, b) = \int_a^\infty \frac{1}{t^L} \exp\left\{-\left(\frac{z}{t} + \frac{t}{b}\right)\right\} dt, \quad (28)$$

where  $z \geq 0$ ,  $a \geq 0$ , and  $b \geq 0$ . This function (28) is closely related to incomplete Bessel function [16]. While  $L$  can be any real number, for our purpose we will assume it to be a positive integer. Since we assume  $a$  and  $b$  to be constants, when it is unambiguous, we will denote  $\mathcal{I}_L(z; a, b)$  by  $\mathcal{I}_L(z)$ . It is easy to verify that  $\mathcal{I}_L(z)$  is a positive, decreasing function; and its values at zero and infinity are given by

$$\mathcal{I}_L(0) = \frac{1}{a^{L-1}} \mathcal{E}_L\left(\frac{a}{b}\right) \quad \text{and} \quad \mathcal{I}_L(\infty) = 0, \quad (29)$$

where  $\mathcal{E}_n(x) = x^{n-1} \int_x^\infty t^{-n} e^{-t} dt = x^{n-1} \Gamma(1-n, x)$  is the generalized exponential integral function [17, Ch. 8.19].

The  $\mathcal{I}_L(z)$  has the following limiting forms [15]:

$$\lim_{a \rightarrow 0} \mathcal{I}_L(z) = \frac{2}{(bz)^{\frac{L-1}{2}}} \mathcal{K}_{L-1}\left(2\sqrt{\frac{z}{b}}\right), \quad (30)$$

$$\lim_{b \rightarrow \infty} \mathcal{I}_L(z) = \frac{1}{z^{L-1}} \gamma\left(L-1, \frac{z}{a}\right), \quad (31)$$

where  $\mathcal{K}_\nu$  is the  $\nu$ -th order modified Bessel function of the second kind. Likewise,  $\lim_{a \rightarrow \infty} \mathcal{I}(z) = \lim_{b \rightarrow 0} \mathcal{I}(z) = 0$ .

The derivative of  $\mathcal{I}_L(z)$  is  $\mathcal{I}'_L(z) = -\mathcal{I}_{L+1}(z)$ , which can be used with (29) to obtain the Taylor expansion of  $\mathcal{I}_L(z)$  at the origin as [15]

$$\mathcal{I}_L(z) = \sum_{n=0}^{\infty} \frac{(-1)^n}{a^{L+n-1}} \mathcal{E}_{L+n}\left(\frac{a}{b}\right) \frac{z^n}{n!}. \quad (32)$$

From (28) and (30), we clearly have the inequality

$$\mathcal{I}_L(z) \leq \frac{2}{(bz)^{\frac{L-1}{2}}} \mathcal{K}_{L-1}\left(2\sqrt{\frac{z}{b}}\right). \quad (33)$$

We can also derive a lower and an upper bound as follows: In the definition (28), since  $e^{-z/a} \leq e^{-z/t} \leq 1$ , we have the lower bound

$$\mathcal{I}_L(z) \geq e^{-z/a} \int_a^\infty \frac{1}{t^L} e^{-t/b} dt = \frac{e^{-z/a}}{a^{L-1}} \mathcal{E}_L\left(\frac{a}{b}\right). \quad (34)$$

Note that (34) is exact at  $z = 0$ . Similarly, since  $e^{-a/b} \geq e^{-t/b}$ , we have an upper bound as

$$\mathcal{I}_L(z) \leq e^{a/b} \int_a^\infty \frac{e^{-z/t}}{t^L} dt = \frac{e^{-a/b}}{z^{L-1}} \gamma\left(L-1, \frac{z}{a}\right). \quad (35)$$

Note that (35) is infinite when  $L = 1$ . Thus, from (34) and (35) we have the inequality for  $\mathcal{I}_L(z)$  as

$$\frac{e^{-z/a}}{a^{L-1}} \mathcal{E}_L\left(\frac{a}{b}\right) \leq \mathcal{I}_L(z) \leq \frac{e^{-a/b}}{z^{L-1}} \gamma\left(L-1, \frac{z}{a}\right). \quad (36)$$

For small values of  $z$ , the relative error of the two bounds in (36) are small; but the relative error increase as  $z$  increases. In contrast, (33) is best for large values of  $z$ , in the sense that its relative error goes to zero as  $z$  increase. These three bounds can be used as approximations to  $\mathcal{I}_L(z)$ . Note that these inequalities have not appeared in [15].

#### REFERENCES

- [1] J. D. Griffin and G. D. Durgin, "Complete link budgets for backscatter-radio and RFID systems," *IEEE Antennas and Propagation Mag.*, vol. 51, no. 2, pp. 11-25, Apr. 2009.
- [2] V. Liu, *et al.*, "Ambient backscatter: wireless communication out of thin air," *ACM SIGCOMM Computer Commun. Review*, vol. 43, no. 4, pp. 39-50, Oct. 2013.
- [3] V. H. Nguyen, *et al.*, "Ambient backscatter communications: A contemporary survey," *IEEE Communications Surveys & Tutorials*, vol. 20, no. 4, pp. 2889-2922, Fourthquarter 2018.
- [4] W. Liu, *et al.*, "Next generation backscatter communication: systems, techniques, and applications," *EURASIP J. Wireless Commun. and Networking*, vol. 2019, no. 69, pp. 1-12, 2019.
- [5] X. Lu, *et al.*, "Ambient backscatter assisted wireless powered communications," *IEEE Wireless Communications*, vol. 25, no. 2, 170-177, Apr. 2018.
- [6] G. Wang, *et al.*, "Ambient backscatter communication systems: Detection and performance analysis," *IEEE Trans. Commun.*, vol. 64, no. 11, pp. 1-10, Aug. 2016.
- [7] G. Yang and Y.-C. Liang, "Backscatter communications over ambient OFDM signals: Transceiver design and performance analysis," *2016 IEEE Global Communications Conference (GLOBECOM)*, pp. 1-4, 4-8 Dec., 2016.
- [8] Y. Liu *et al.*, "Coding and detection schemes for ambient backscatter communication systems," *IEEE Access*, vol. 5, no. 99, pp. 4947-4953, Mar. 2017.
- [9] J. Qian, *et al.*, "Noncoherent detections for ambient backscatter system," *IEEE Trans. Wireless Commun.*, vol. 16, no. 3, pp. 1412-1422, Mar. 2017.
- [10] J. Qian, *et al.*, "Semi-coherent detection and performance analysis for ambient backscatter system," *IEEE Trans. Wireless Commun.*, vol. 65, no. 12, pp. 5266-5278, Dec. 2017.
- [11] Q. Tao, *et al.*, "Symbol detection of ambient backscatter systems with Manchester coding," *IEEE Trans. Wireless Commun.*, vol. 17, no. 6, pp. 4028-4038, Jun. 2018.
- [12] G. Yang, *et al.*, "Modulation in the air: Backscatter communication over ambient OFDM carrier," *IEEE Trans. Commun.*, vol. 66, no. 3, pp. 1219-1233, Mar. 2018.
- [13] M. A. ElMossallamy, *et al.*, "Noncoherent backscatter communications over ambient OFDM signals," *IEEE Trans. Commun.*, vol. 67, no. 5, pp. 3597-3611, May 2019.
- [14] D. Darsena, "Noncoherent detection for ambient backscatter communications over OFDM signals," *IEEE Access*, vol. 7, 2019.
- [15] S. Guruacharya, B. K. Chalise, and B. Himed, "On the product of complex Gaussians with applications to radar," *IEEE Signal Process. Lett.*, vol. 26, no. 10, pp. 1536-1540, Oct. 2019
- [16] F. E. Harris, "Incomplete Bessel, generalized incomplete gamma, or leaky aquifer functions," *J. Computational and Applied Math.*, vol. 215, no. 1, pp. 260-269, 15 May 2008.
- [17] F. W. J. Olver, D. W. Lozier, R. F. Boisvert, and C. W. Clark, *NIST Handbook of Mathematical Functions*, Cambridge University Press, New York, NY, 2010. Print companion to *NIST Digital Library of Mathematical Functions (DLMF)*: <http://dlmf.nist.gov/>, Release 1.0.11 of 2016-06-08.